Astron. Astrophys. 358, 321–331 (2000)

ASTRONOMY AND ASTROPHYSICS

Modeling emission lines of 8 northern planetary nebulae⋆

C. Neiner[1,2], A. Acker[1], K. Gesicki[3], and R. Szczerba[4]

[1] Observatoire de Strasbourg, 11, rue de l'université, 67 000 Strasbourg, France (acker@astro.u-strasbg.fr)
[2] Observatoire de Paris-Meudon, 5, place Jules Janssen, 92195 Meudon Cedex, France (Coralie.Neiner@obspm.fr)
[3] Centrum Astronomii UMK, ul. Gagarina 11, 87-100 Toruñ, Poland (gesicki@astri.uni.torun.pl)
[4] Nicolaus Copernicus Astronomical Center, ul. Rabianska 8, 87-100 Toruñ, Poland (szczerba@ncac.torun.pl)

Received 21 January 2000 / Accepted 11 April 2000

Abstract. In order to constrain the nebular density distribution and velocity field, we model nebular lines profiles obtained at very high spectral resolution. The method and computer code applied to 2–3 nebular lines were described in earlier publications. In the present work we analyse 4–11 spectral lines observed simultaneously with the spectrometer ELODIE (R=42 000) for 8 planetary nebulae. For five analyzed nebulae with a [WC]-type nucleus, we found highly broadened profiles implying possible turbulent motions.

Key words: ISM: planetary nebulae: general – turbulence – stars: Wolf-Rayet

1. Introduction

Planetary nebula (PN) morphology and dynamics reflect the mass-loss history of the associated proto-white dwarf, central star.

In order to determine the nebular velocity field, we observed nebular line profiles at very high spectral resolution, and modeled them. The method and computer codes applied to the [O III], [N II] and H I lines of three PNe with O-type nuclei have been published by Gesicki et al. (1996) - hereafter refered to as Paper I. In a second paper, we analysed three nebulae around [WC] stars (see Gesicki & Acker, 1996). We found that nebular emission lines show highly broadened profiles implying possible turbulent motions. This conclusion should be checked (i) among more [WC] and O-type central stars of PNe, (ii) using more spectral lines to allow a deeper exploration of the ionized nebular structure. In this context, we have carried out observations with the spectrometer ELODIE at the "Observatoire de Haute-Provence" (OHP).

2. The observational data

2.1. The observations

The observations were carried out with the 1.93m telescope at the OHP in France, equiped with the ELODIE spectrograph. This spectrograph (described by Baranne et al., 1995) uses cross-dispersion with a fixed optical system. It is illuminated by a pair of fibres from the Cassegrain focus.

The spectra were obtained in March 1998 with a circular aperture of 2″diameter on the sky. These echelle spectra cover a wavelength domain from 3906 to 6811 Å, distributed over 67 orders. The resolution power is R=42 000, with instrumental broadening ≃ 0.1 Å in the direct fibre mode.

Extraction of the spectra is completely included within the spectrograph control: bias, flat-field, cosmic rays, bad pixels, Earth motion corrections and wavelength calibration with a thorium-argon source. However, as the spectrograph is dedi-

Table 1. Journal of observations

Nebula	Type	Date	Expos.	X	S/N
		06.03.98	1800 s	1.12	32
NGC 6543	[WC] -	07.03.98	1800 s	1.17	4
96.4+29.9	PG1159	08.03.98	2700 s	1.25	14
	(A)	09.03.98	900 s	1.11	9
		09.03.98	3600 s	1.49	3
NGC 1501	[WC4]	09.03.98	3600 s	1.74	3
144.5+6.5	(A)	09.03.98	3600 s	2.07	2
		10.03.98	3600 s	1.53	6
		10.03.98	3600 s	1.78	5
		06.03.98	1800 s	2.23	14
NGC 40	[WC8]	06.03.98	1800 s	2.22	11
120.0+9.8	(A)	07.03.98	3600 s	2.18	14
		07.03.98	3600 s	2.23	13
BD +303639	[WC9]	09.03.98	3600 s	1.45	3
64.7+5.0	(A)				
M 4–18	[WC11]	08.03.98	5400 s	1.77	8
146.7+7.6	(A)	08.03.98	5400 s	2.33	6
NGC 3242	O(H)	06.03.98	3600 s	2.21	9
261.0+32.0	(M)				
IC 418	Of(H)	08.03.98	3600 s	2.00	32
215.2-24.2	(M)	09.03.98	3600 s	2.11	20
		09.03.98	900 s	2.22	7
IC 2165	(?)	06.03.98	3600 s	2.10	5
221.3-12.3		10.03.98	3600 s	2.03	4

References: A = Acker et al., 2000; M = Mendez et al., 1991

Send offprint requests to: A. Acker

⋆ Based on observations taken at the Observatoire de Haute-Provence du CNRS

Table 2. Line ratios

	NGC 6543	NGC 1501	NGC 40	BD +30 3639	M 4–18	NGC 3242	IC 418	IC 2165	Mean
[N II] $\frac{6583}{6548}$	3.02	3.37	2.98	2.16	3.16	-	3.00	3.00	2.96 ± 0.14
[O III] $\frac{5007}{4959}$	2.55	-	-	2.93	-	2.97	2.33	3.90	2.94 ± 0.33
[S II] $\frac{6717}{6732}$	0.64	0.68	0.66	0.44	0.51	0.73	0.51	0.58	

Table 3. Lines modeled with the computer codes (χ_i is the ionisation potential)

Line	Hβ	He II	[N I]	[N I]	[N II]	[O I]	[O III]	[Ne III]	[Ne IV]	[S II]	[S III]	[Cl III]	[Ar IV]	[Ar V]
λ (Å)	4861	4686	5198	5201	6585	6302	5008	3968	4725	6732	6311	5518	4711	6435
Order	31	27	40	40	64	60	35	3	28	66	60	46	27	62
χ_i (eV)	13.6	54.4	14.5	14.5	29.6	13.6	54.9	63.4	97.2	23.4	34.7	39.9	59.8	75.0
N	9	3	3	2	8	6	7	6	1	7	5	3	4	1

N = number of observed nebulae

cated to radial velocity mesurements, flux calibration is not done automatically. Our main aim was to obtain line profiles. In addition, we have also attempted to obtain the relative intensity of the lines, in order to calculate some plasma parameters needed for the code. Therefore, the spectrophotometric standard star HD 93521 was observed daily. The calibration was carried out in the Midas environment. We calculated a response curve for each order, by using HD 93521's theorical spectrum (flux given with 1 Å step, see Oke, 1990).

Eight planetary nebulae have been analysed: 5 with a [WC] nucleus, 2 having an O-type central star, and another lacking a spectral type. They are listed in Table 1. Column 1 gives the usual name of the nebula, followed by the galactic designation from Acker et al. (1992). Column 2 presents the spectral type of the nucleus. The date of observation, the exposure time and the airmass value are given in Columns 3,4 and 5, respectively. Column 6 gives the signal-to-noise ratio (S/N) as calculated by ELODIE, averaged over the whole spectrum. The S/N of the bright emission lines used in our modelization is very high, up to 500.

We observed the region of the nebula centered on the nucleus. If several spectra were observed for the same object, we calculated a mean spectrum as follows:

$$S_{\rm mean} = \sum_{\rm i=1}^{\rm N} \alpha_{\rm i} S_{\rm i} \Big/ \sum_{\rm i=1}^{\rm N} \alpha_{\rm i}, \qquad (1)$$

where α_i is S/N for spectrum S_i.

For the brightest nebulae, two spectra with a different exposure time are needed: a short exposure for the most intense lines and a longer exposure allowing the good analysis of most fainter lines.

2.2. Reliability of the data

We check the intensity ratios of the [N II] and [O III] doublets, for which the theoretical ratios are 2.94 and 2.88, respectively (see Mendoza, 1983). As shown in Table 2, the results seem acceptable for the [N II] doublet, for which the lines belong to the same order (64), but they are less precise for [O III] (lines situated in the orders 34 and 35)(see Osterbrock, 1989)

Therefore, we use only intensity ratios of lines belonging to the same order. The ratio of the intensities of the [S II] doublet (order 67) (see Table 2) allows us to determinate the electron density.

3. Modeling of the selected nebulae

3.1. The computer codes

The computer codes applied for nebulae modelling are described in details in Paper I. Therefore we present in this section only a very short description of the calculations which are performed in two steps.

First the photoionization structure is calculated. The nebula is approximated as a spherical shell defined by inner and outer radii, total mass, radial density distribution, radial velocity field, chemical composition. It is ionized by the central star with assumed luminosity and effective temperature. The free parameters are adjusted to obtain as good as possible agreement between the observed and calculated values of: flux in Hβ, line ratios, plasma parameters. Also monochromatic images are taken into account for deducing the density distribution.

In the second step the spectral line emission coefficients resulting from photoionization equilibrium are integrated over the nebula, in order to obtain spectral line shapes. Comparison of these lines with observations allows to correct the assumed velocity field. In this step the spectral resolution, the instrumental profile and seeing conditions are taken into account. When all calculated lines remain still too narrow to fit the observations, a turbulent broadening is introduced to the model.

As we precise in our earlier papers, the fits cannot be considered as unique. We try to find a model which is as simple as possible and satisfactory reproduces the observed nebula, taking into account the limitations of the spectral resolution of our observations and the simplicity of our model. Therefore we as-

Table 4. Chemical compositions

	NGC 6543 this work	NGC 1501 this work	NGC 40 P91	BD +30 3639 P86	M 4–18 S95	NGC 3242 AC93	IC 418 G96	IC 2165 G96
He	11.05	11.04	10.95	11.04	10.99	10.95	11.20	11.04
C	9.10	8.89	8.81	8.6	8.56	8.43	8.30	9.10
N	7.94	8.39	7.99	7.76	8.08	7.91	7.60	7.97
O	8.75	8.65	8.70	8.4	9.23	8.66	8.40	8.73
Ne	8.15	8.01	7.50	8.01	8.09	7.85	7.49	8.01
Mg	5.95	5.95	5.95	6.6	5.95	5.95	5.95	5.95
Si	6.76	6.76	6.76	6.3	6.76	6.76	6.76	6.76
S	7.00	7.04	7.04	6.8	6.00	6.69	7.00	7.04
Cl	5.47	5.32	5.32	5.32	5.32	5.06	5.18	5.32
Ar	6.42	6.46	6.46	6.46	6.56	6.26	6.70	6.46

For all the PN: H=12.00, Na=6.18, K=4.95, Ca=5.03

References: For all the PN Aller & Czyzak, 1983, corrected by: AC93 = Aller & Czyzak, 1993; G96 = Gesicki et al., 1996 (Paper I); P86 = Pwa et al., 1986; P91 = Perinotto, 1991; S95 = Surendiranath & Kameswara Rao, 1995

Table 5. Data from the literature and adopted for modeling for the PNe (references are given in brackets)

PN G	NGC 6543 96.4+29.9	NGC 1501 144.5+6.5	NGC 40 120.0+9.8	BD +30 3639 64.7+5.0	M 4–18 146.7+7.6
distance [kpc]					
literature (Z)	1.12	1.48	1.21	1.85	6.85
model	*1.12*	*1.2*	*1.24*	*2.6*	*6.8*
NEBULA					
angular diameter [arcsec]					
literature: optical	19.5 (CGPN)	52 (CGPN)	48 (CGPN)	4.5 (mean)	3.5 (mean)
model	*18.4*	*55.0*	*46.6*	*5.6*	*3.64*
external radius [pc] (model)	*0.05*	*0.16*	*0.14*	*0.035*	*0.06*
electron temperature [K]					
literature	8300(P)		8500(P)	8000(P)	6600(S95)
model from [O III] ([N II])	*8340(8500)*	*13000(13000)*	*7520(7400)*	*8600(8410)*	*6650(6580)*
log electron density [cm^{-3}]					
OHP observations (this work)	3.34	3.28	3.30	4.08	3.67
literature	3.77(O)		3.11(P)	4.00(P)	3.78(S95)
model	*3.90*	*3.17*	*3.07*	*4.15*	*3.55*
log F(Hβ)					
literature (CGPN)	−9.58	−10.08	−10.14	−9.67	−10.99
model	*−9.06*	*−9.91*	*−9.66*	*−9.78*	*−11.00*
extinction literature (mean)	0.03	1.2	0.52	0.36	0.9
ionized mass [$M_\odot$] (model)	*0.12*	*0.18*	*0.25*	*0.08*	*0.1*
exp. velocity O III (N II) [$km\,s^{-1}$]					
literature (CGPN)	19.5(20)	37	29(26)	23(28)	7.5(17)
model	*17*	*40*	*25*	*27*	*15*
turbulence [$km\,s^{-1}$] (model)	*12*	*10*	*8*	*15*	*15*
STAR					
magnitude V (CGPN)	11.14	14.39	11.58	11.8	13.96
spectral type (A)	[WC] PG1159	[WC4]	[WC8]	[WC9]	[WC11]
log(T_{eff}) [kK]					
literature	4.66 (S)	-	4.52 (ZK)	4.49 (ZK)	4.48(L)
model	*4.70*	*5.15*	*4.52*	*4.41*	*4.40*
log($L/L_\odot$)					
literature	3.59 (S)	-	3.60 (ZK)	4.1 (Z93)	3.67 (L)
model	*3.60*	*3.8*	*3.30*	*4.1*	*3.80*

References: A = Acker et al., 2000; CGPN = Acker et al., 1992; G = Gorny et al., 1997; L = Leuenhagen et al., 1996; M1 = Mendez et al., 1991; M2 = Mendez et al., 1992; O = Osterbrock, 1989; P = Pottasch, 1984; S = Stasinska et al., 1997; S95 = Surendinarath & Kameswara Rao, 1995; Z = Zhang, 1995; ZK = Zhang & Kwok, 1993; Z93 = Zhang, 1993

	NGC 3242	IC 418	IC 2165
PN G	261.0+32.0	215.2-24.2	221.3-12.3
distance [kpc]			
literature (Z)	0.94	1.02	2.52
model	*1.0*	*1.02*	*2.5*
NEBULA			
angular diameter [arcsec]			
literature: optical	38 (M2)	14.4 (mean)	7.7 (mean)
model	*41.3*	*14.6*	*7.8*
external radius [pc] (model)	*0.1*	*0.036*	*0.057*
electron temperature [K]			
literature	11000(P)	9700(O)	13000(P)
*model from [*O III*] ([*N II*])*	10090(9940)	9500(9590)	11790(11270)
log electron density [cm^{-3}]			
OHP observations (this work)	3.45	3.98	3.51
literature	3.20(O)	4.15(P)	3.70(P)
model	3.14	4.12	3.26
log F(Hβ)			
literature (CGPN)	-9.70	-9.45	-10.39
model	*-9.68*	*-9.45*	*-10.25*
extinction literature (mean)	0.09	0.05	0.5
ionized mass [$M_\odot$] (model)	*0.15*	*0.05*	*0.076*
exp. velocity O III (N II) [$km\,s^{-1}$]			
literature (CGPN)	20(27.5)	26(12)	20
model	*31*	*15*	*25*
turbulence [$km\,s^{-1}$] (model)	*no*	*no*	*14*
STAR			
magnitude V (CGPN)	12.31	10.17	17.9
spectral type (M1)	O(H)	Of(H)	?
log(T_{eff}) [kK]			
literature	4.74 (G)	4.57 (G)	5.20 (G)
model	*4.90*	*4.57*	*5.19*
log($L/L_\odot$)			
literature	3.31 (G)	3.92 (Z93)	3.56 (G)
model	*3.30*	*3.92*	*3.20*

sume the expansion velocity either constant or changing very smoothly with radius. Nevertheless it is relatively straightforward to accurately fit a single spectral line. Simultaneous fitting of more lines gives more constraints to the model. The emission coefficients in different lines have a different radial distribution, therefore more lines give more probes across the nebula. In earlier papers we considered three spectral lines, namely Hα, [OIII] and [NII], which we considered as a minimum set. Our new observations provide more lines and made our analysis more reliable. The codes compute 94 ionization stages of 14 elements (see Paper I) and we choose 14 lines originating from different regions of the nebulae following a stratification versus the ionisation potential (see Table 3). Lines with high values of the potential are emitted by ions situated close to the central star, whereas lines with low potential values come from external zones probably with fast expansion. So, 14 lines were compared to the observations, but only the brightest ones (from 4 to 11 lines per nebulae) were used for final calculations.

3.2. Analysis of the selected nebulae

Eight planetary nebulae were studied. Tables 5 give the values of the parameters adopted in our modelisation (shown in italics), and compared to the values taken from the literature and used for the first iterations. For log F(Hβ), we give the value from CGPN corrected by the mean extinction coefficient. Note that in two cases (NGC 6543 and NGC 40), there is a discrepancy between literature and model: as many parameters must be adjusted at the same time, these are the best compromises found. For the expansion velocity derived from our modelisation, we give the constant value adopted in some cases, or the mass weighted average value computed as described in Gesicki et al., 1998. For determination of N_e and T_e, we have used ratios of [S II] 6717/6732 (N_e), [O III] (4959+5007)/4363 and [N II] (6548+6583)/5755 (T_e). We have plotted the diagnostic curves (see e.g. Aller 1984) on the T_e-N_e diagram and as the values given in the table we used the numbers resulting from the intersections of the appropriate lines. For all objects, the electron

Table 6. Comparison of observed and calculated line ratios relative to (Hβ) = 100

	NGC 6543			NGC 1501			NGC 40		
Line	MP89	BC74	model	SK94	K76	model	CS83	K76	model
He II 4686			0.2	35.1	38.2	111			-
[N I] 5198			0.2			-	0.7		0.4
[N II] 6585	19.5		92.1	31.0		32.8	298		192
[O I] 6302			1.2			-	3.1	16.5	1.5
[O II] 3729	15.8	8.9	33.5	50.1		14.1		134	104
[O III] 5008	787		457	1306	987	1476	17.9	28.4	16.1
[Ne III] 3869	55.4		33.0	133	86.4	124	0.3	0.7	0.2
[Ne III] 3968	32.9	37.0	10.2	44.0	30.5	38.4	14.6	0.7	-
[S II] 6732			6.6	8.2		0.7	14.7	43.1	35.1
[S III] 6311			1.8			1.8	0.6		0.8
[Cl III] 5518			0.4			-	0.3		0.3
[Ar IV] 4711		1.4	0.9			19.8			-

	BD +30 3639			M 4–18			
Line	R91	P71	model	S80	GD85	K83	model
He II 4686			-				-
[N I] 5198		0.7	-				0.2
[N II] 6585	407	361	1380	212		150	155
[O I] 6302	4.3	2.6	0.6		3.4		2.3
[O II] 3729			23.9		332.3	106	99.3
[O III] 5008		3.9	8.4	5.2			4.6
[Ne III] 3869			0.2				-
[Ne III] 3968			-				-
[Ne V] 3426			-				-
[S II] 6732	28.1		7.9	28.1	22.1		1.7
[S III] 6311			1.0				-
[Ar IV] 4711			-				-

	NGC 3242			IC 418			IC 2165		
Line	P94	B85	model	H94	GM85	model	HA94	GM85	model
He II 4686	47.4	45.2	13.9		0.2	-	62.6	41.7	44.1
[N I] 5198				0.4		-	0.2		0.5
[N II] 6585	40.1		7.0	206.8		104.2	19.3		79.2
[O I] 6302				3.9		0.8	1.4		4.9
[O II] 3729		2.8	9.0	37.7		35.4	8.9		63.7
[O III] 5008	1009	1230	1220	85.9	151	149.5	1181	1349	1622
[Ne III] 3869	122	96.9	78.5	2.1		5.7	81.9		143.5
[Ne III] 3968	44.1		24.2	0.6		1.8	24.6		44.3
[Ne V] 3426		5.0	0.1		0.4	-		49	52.4
[S II] 6732	0.3	0.1	0.2	6.8		8.2	1.5		8.9
[S III] 6311	0.6	0.4	0.4	0.9		3.3	1.5		3.0
[Ar IV] 4711	6.4	5.1	8.2			0.8	5.2		8.4

- = less than 0.1

References: B85 = Barker, 1985; BC74 = Boeshaar & Czyzak, 1974; CS83 = Clegg et al., 1983; GD85 = Goodrich & Dahari, 1985; GM85 = Gutierrez-Moreno et al., 1985; H94 = Hyung, 1994; HA94 = Hyung, Aller & Feibelman, 1994; K76 = Kaler, 1976; K83 = Kaler, 1983; MP89 = Manchado & Pottasch, 1989; P71 = Peimbert & Torres-Peimbert, 1971; P94 = Perinotto et al., 1994; R91 = Rudy et al., 1991; S80 = Sabaddin, 1980; SK94 = Stanghellini, Kaler & Shaw, 1994

density resulting from two intersections is the same, slightly different are the electron temperature determinations.

Table 6 compares the line ratios calculated by the code with those taken from the literature, all these ratios being dereddened and given relative to I(Hβ)=100. In some cases, the calculated line ratios differ from observed values by a factor up to 2–3. This stems from the approximate assumption of blackbody ionizing radiation combined with poorly known chemical composition and density structure. As in Paper I, the mean chemical composition given by Aller & Czyzak, 1983, was used, supplemented

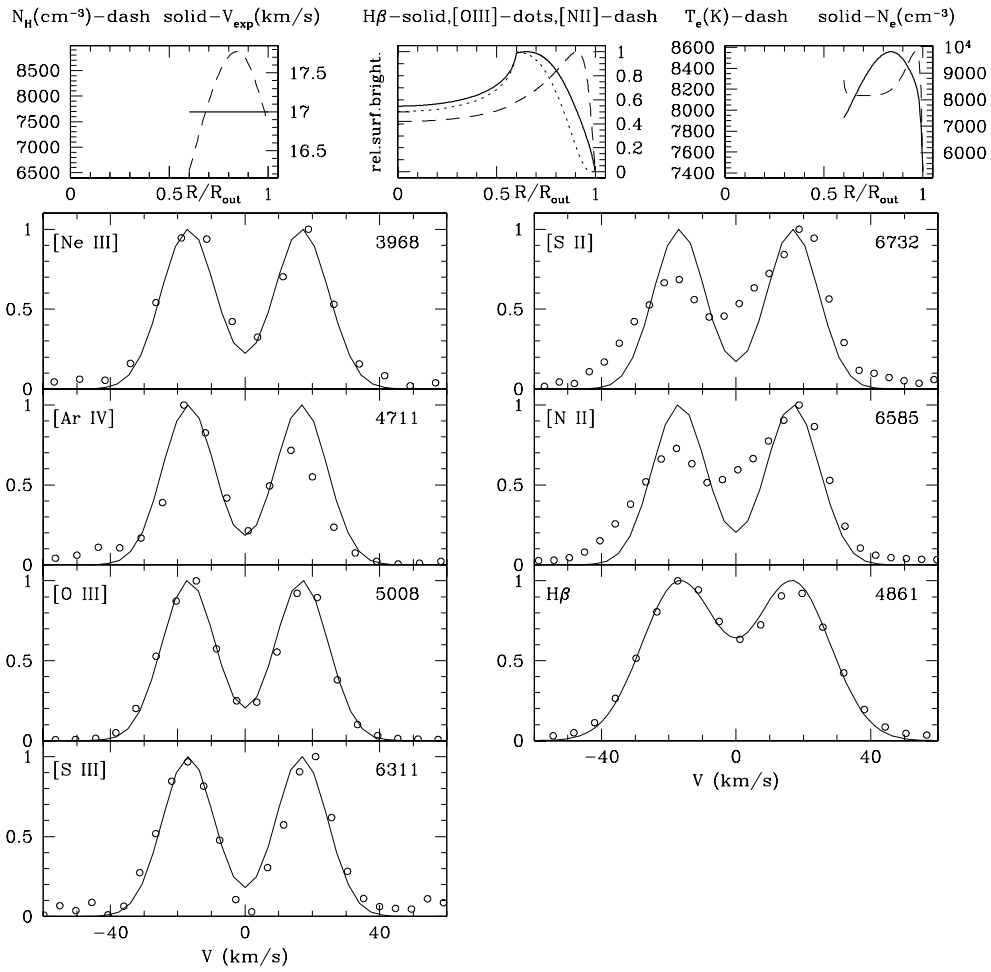

Fig. 1. Comparison between observations and modelisation for NGC 6543 [WC] PG1159

by values given in the literature for specific PNe, or our own values (Table 4). In principle, it was possible for us to find our own values of chemical composition for each nebula analyzed, but this is beyond the scope of the present paper.

Figs. 1 to 5 show the results for the five PNe with [WC] central stars and Figs. 6 to 8 for other type stars. The modeled profiles are given by solid lines, the observations by circles. When the PN has already been analyzed in Paper I, the old observations are given by black points. The 3 graphs on the top of each figure show the velocity field and the density distribution, the relative surface brightness for Hβ, [O III] and [N II], and the electron temperature and density, as a function of the normalized PN radius. Note that there is a disagreement between N_e and N_H in some cases, when one could expect that these quantities vary in step. This is due to helium: the electrons from ionized helium increase N_e as seen for NGC 3242 or IC 2165, and the recombination explains the wiggle in the N_e distribution as seen for BD +30 3639, M 4–18 or IC 418. The next boxes show the different lines classified by decreasing ionisation potential.

"Turbulence" (i.e. non-zero turbulent velocity) is needed when all the lines are strongly broadened, whatever the value of the atomic mass and the region in which they are formed is. In the example of NGC 3242, we can see (i) the H-lines enlarged by thermal broadening (about 4 times higher than for the heavy O and N ions) and (ii) higher expansion velocity for line emission coming from external regions of the nebula. As expected, no turbulent velocity was necessary for this object. On the contrary, it is clear that all the lines in BD +30 3639, with a [WC] nucleus, are broadened by the turbulence.

As shown in Table 5, non-zero turbulent velocity was necessary to model PNe with a [WC] central star. PNe with O-type stars do not require a finite turbulent velocity but show an increasing velocity field. These results have already been considered by Gesicki & Acker (1996).

4. Discussion

NGC 6543 ([WC]–PG1159): The 7 lines (Fig. 1) are well modeled using a parabolic density variation (in agreement with the monochromatic images of Balick 1987), and constant velocity field with finite turbulent velocity.

NGC 1501 ([WC4]): This large nebula has a faint surface brightness. Therefore, only 4 spectral lines are well observed (Fig. 2). The models match well with the observations for all of them. Nevertheless, some finite turbulent velocity was added to the high expansion velocity to obtain a good fit. The image given in Manchado et al. (1996) shows spherical symmetry but also

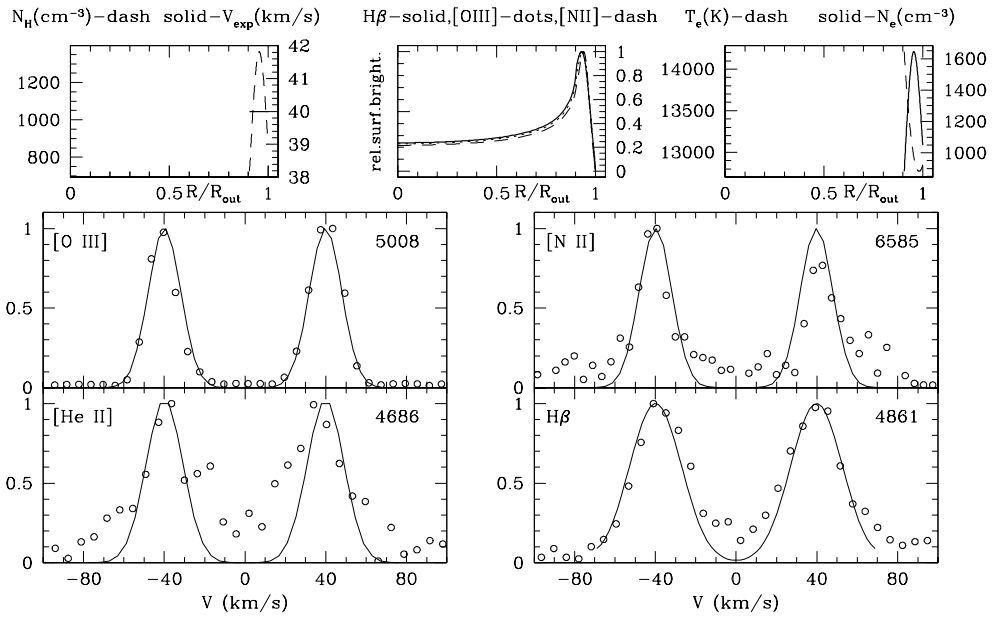

Fig. 2. Comparison between observations and modelisation for NGC 1501 [WC4]

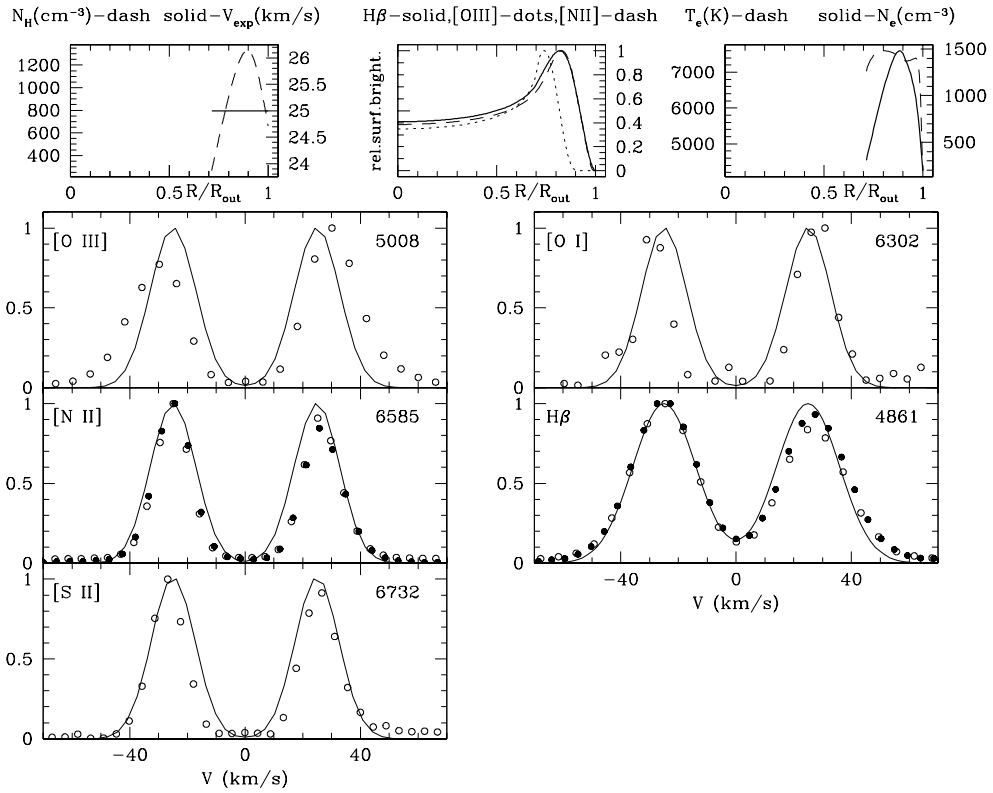

Fig. 3. Comparison between observations and modelisation for NGC 40 [WC8]

clumpy structures. The model is density bounded, as expected for evolved nebulae with a cooled nucleus.

NGC 40 ([WC8]): This PN (Fig. 3) has already been modeled using our code applied to 3 lines (see Gorny et al., 1997). Two possibilities were suggested: either the velocity field is constant and there is non-zero turbulent velocity, or the velocity field increases with zero turbulent velocity. In this work, 5 lines are well observed, so we can now differentiate the 2 solutions: a finite turbulent velocity is indeed necessary. Moreover, the [O III] line exhibits higher velocity although it forms in the inner nebular region, as given in the literature (see Table 5). Such a peculiar behaviour can be related to external regions compressed by the motion of the star (see Acker et al., 1998). The density distribution varies in agreement with the images done by Balick (1987).

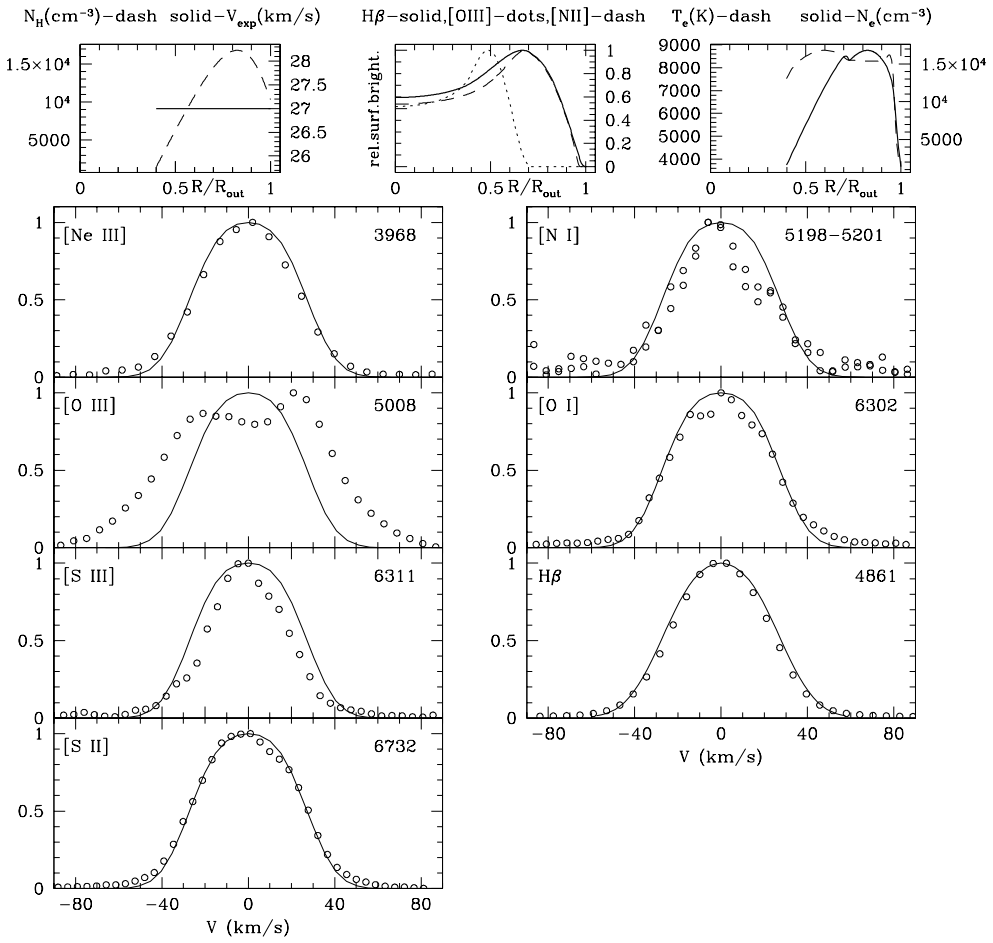

Fig. 4. Comparison between observations and modelisation for BD +30 3639 [WC9]

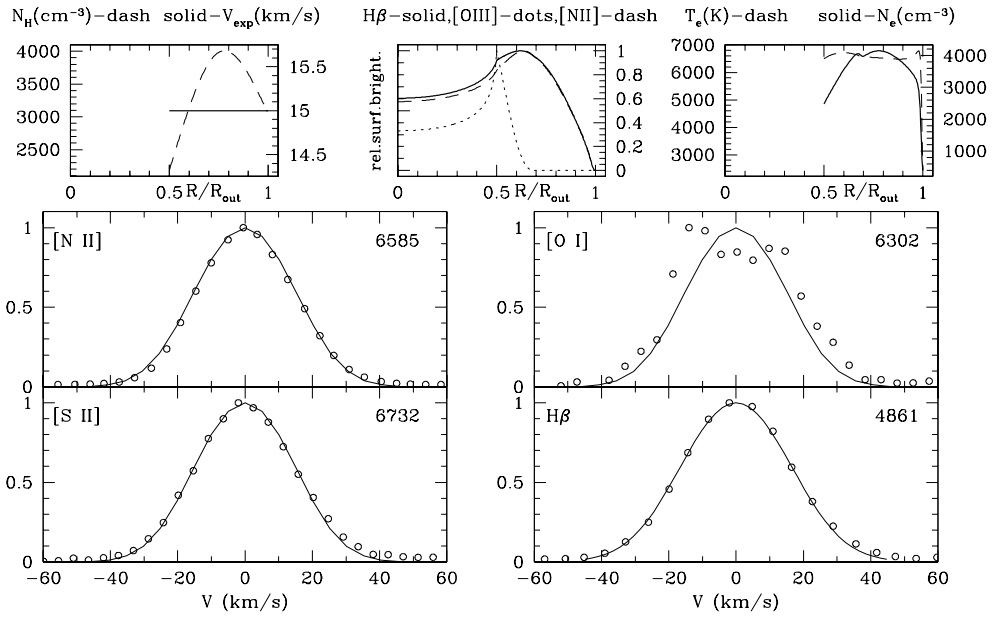

Fig. 5. Comparison between observations and modelisation for M 4–18 [WC11]

BD +30 3639 ([WC9]): This very young nebula is dense and compact. Seven lines are well observed (Fig. 4). With appropriate turbulent velocity, the widths of the lines are well represented, except for the [O III] line. The profile of this line is peculiar, broad and splitted, as already noted by Aller & Hyung (1995) and Sabbadin (1984). The [O III] image presents a bright spot in the center, which is not reproduced by our calculations. The density distribution was defined as suggested by the monochromatic images of Balick (1987), Arnaud et al. (1996)

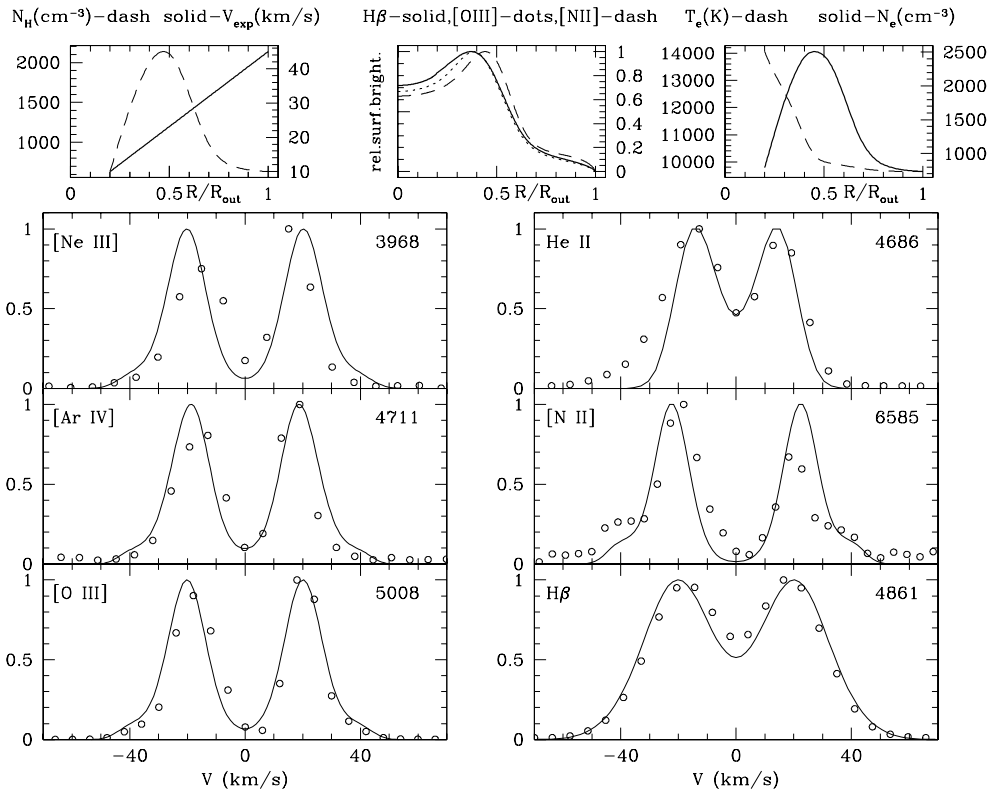

Fig. 6. Comparison between observations and modelisation for NGC 3242 O(H)

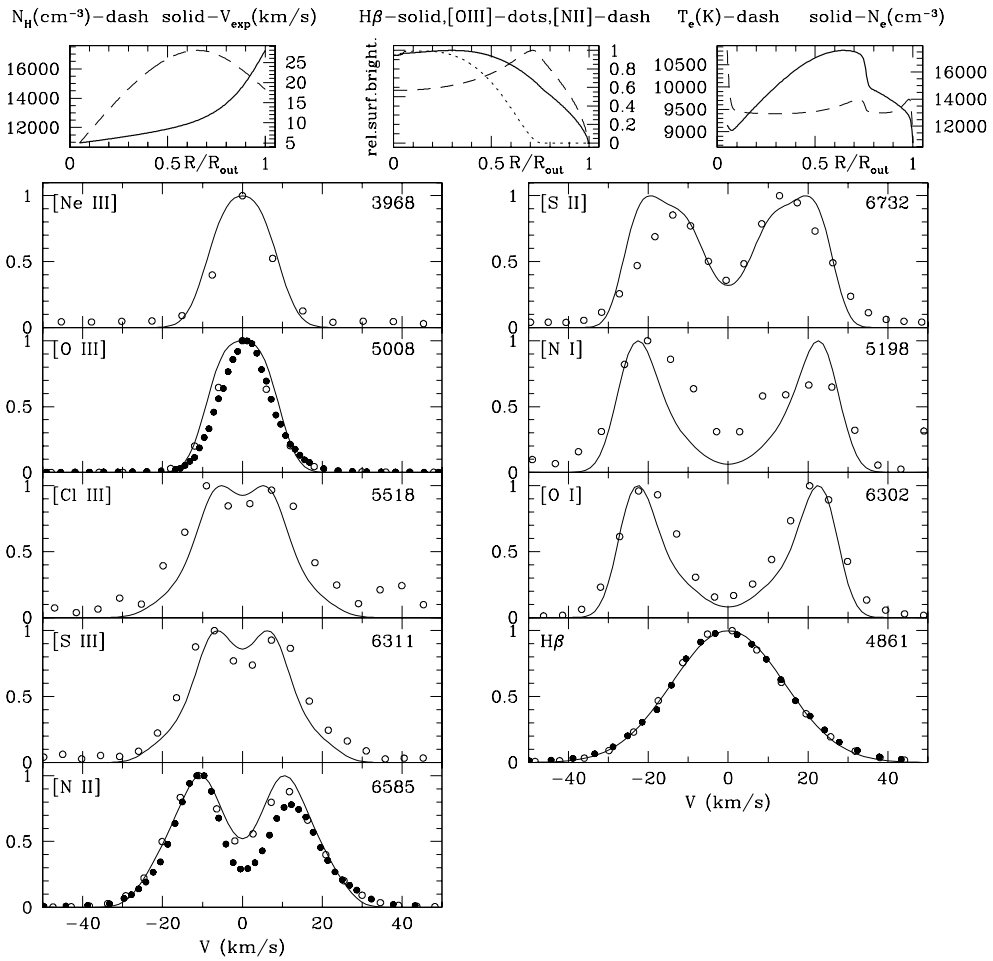

Fig. 7. Comparison between observations and modelisation for IC 418 Of(H)

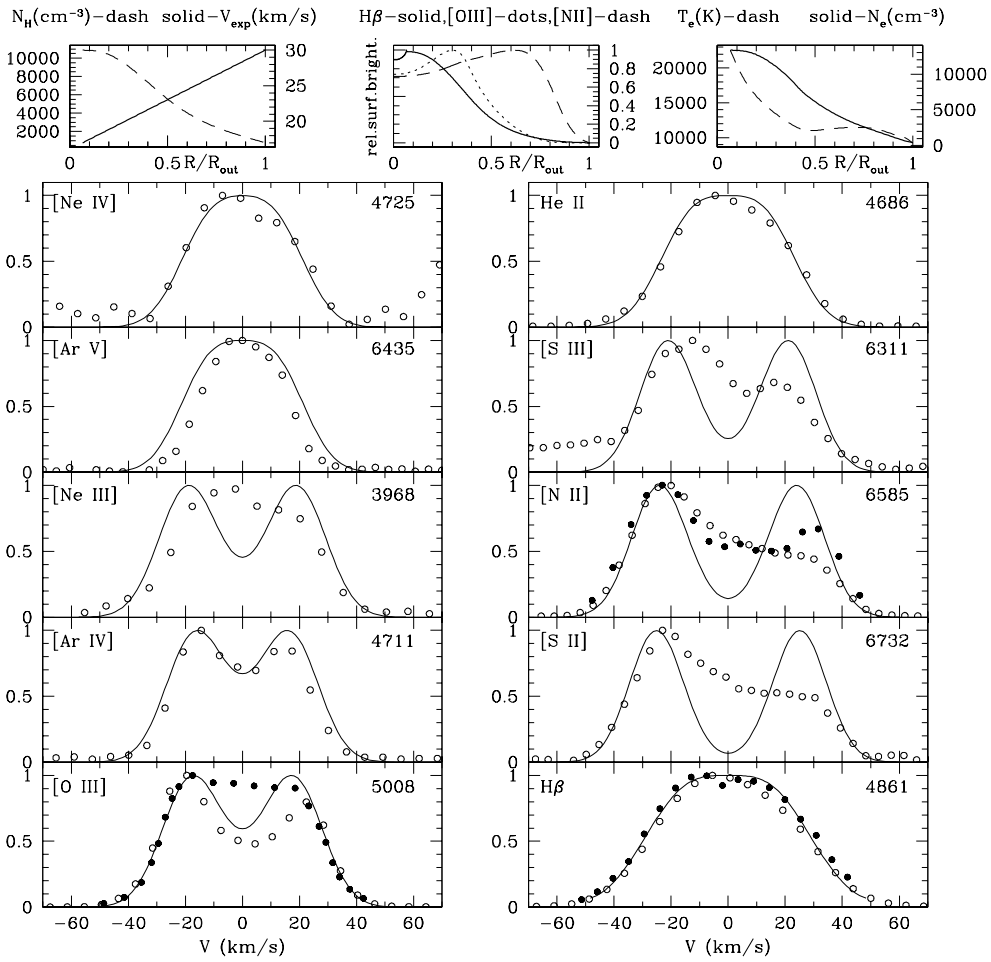

Fig. 8. Comparison between observations and modelisation for IC 2165

and Harrington et al. (1997) which suggest big inner nebular radius.

M 4–18 ([WC11]): Only 4 lines are well observed (Fig. 5), and modeled by adding some finite turbulent velocity. However, the [O I] line should have structures originated in not-ionized, neutral, outer regions, not considered by our photoionization model.

NGC 3242 (O(H)): The 6 observed lines appear splitted (Fig. 6), but the model was difficult to adjust because the lines look asymmetric. We used the monochromatic images given by Balick (1987), and Schwarz et al. (1992). The model used is density bounded. A symmetric "bump" appears in the wings, especially for the [N II] and [O III] lines, and has been well reproduced. This structure could reflect the "true" velocity of the gas (see Schönberner, 1997). Such a phenomenon should be seen in most of the "multiple shell PNe" (classified by Stanghellini et al., 1997).

IC 418 (Of(H)): This nebula was observed and modeled in Paper I. Note that the shape of the new observed lines differ from the old ones: the aperture was centered on a different zone of the nebula. However we decide to use the same parameters as defined in the model already calculated in Paper I. The adopted surface brightnesses are in agreement with the monochromatic images from Balick (1987), and Schwarz et al. (1992). No turbulent velocity was necessary (see Fig. 7). The fit of the brightest lines looks good. For some other lines, the modeling seems difficult to adjust.

IC 2165: This PN was already modeled in Paper I with 3 lines. Ten lines are now well observed (see Fig. 8). The parameters used for the modelisation remain about the same than in Paper I, with a density distribution corresponding to the monochromatic images of Schwarz et al. (1992). We tried to reproduce the small splitting appearing in some lines, like [Ne III] or [Ar IV]. The model considered consist on an increasing velocity field and finite turbulent velocity. This velocity field is simpler than in Paper I, as the splitted profile of [O III] line does no more require a plateau at low velocities. More observations are needed for allowing a more comprehensive description of the unknown spectrum of this nucleus. Observations done by one of us (AA) show an emission of He II 4686 Å being from stellar origin, in addition to the narrow nebular line.

5. Conclusion

The Torun's codes are based on a global and coherent description of the system star plus nebula. By modeling successfully a large number of emission lines originating from very different nebular zones, we can give a more realistic description of the object. Nevertheless, the comparison between new models for IC 418 and IC 2165 and models from Paper I shows that 3 lines give reasonably good conclusion.

From modeling nebular line profiles, we show that turbulent motions should exist in the nebulae with [WC]-type nuclei. Highly broadened profiles could also result from strong variations of the expansion rate in the radial direction relative to the central core, possibly related to anisotropy in the stellar wind.

Moreover, the new analysis confirms our earlier results that PN with non-[WC] nuclei show increasing velocity, but note (i) the exceptional case of IC 2165 with gradient and turbulence, (ii) [O III] lines with higher velocities for NGC 40 and BD +30 3639.

New observations and further work are planned.

Acknowledgements. This project was partially supported by the CNRS in the frames of the JUMELAGE "Astronomie Pologne" programme. K. Gesicki and R. Szczerba acknowledge partial support from Polish KBN grant No. 2.P03D.002.13. The authors would like to thanks Joachim Köppen for his help on electron temperatures and densities.

References

Acker A., Marcout J., Ochsenbein F., Stenholm B., Tylenda R., 1992, Strasbourg-ESO Catalogue of Galactic Planetary Nebulae
Acker A., Fresneau A., Pottasch S.R., Jasniewicz G., 1998, A&A
Acker A., Durand S., Parthasarathy M., Stenholm B., 2000, A&A, submitted
Allen C.W., 1976, Astrophysical quantities. University of London, The Athlone Press
Aller L.H., Hyung S., 1995, MNRAS 276, 1101
Arnaud K., Borkowski K.J., Harrington J.P., 1996, ApJ 462, L75
Balick B., 1987, AJ 94, 671
Baranne A., Queloz D., Mayor M., et al., 1996, A&AS 119, 373
Barker T., 1985, ApJ 294, 193
Boeshaar G.O., Czyzak S.J., Aller L.H., 1975, ApJS 28, 335
Clegg R.E.S., Seaton M.J., Peimbert M., Torres-Peimbert S., 1983, MNRAS 205, 417
Gesicki K., Acker A., Szczerba R., 1996, A&A 309, 907 (Paper I)
Gesicki K., Acker A., 1996, Ap&SS 238, 101
Gesicki K., Acker A., Zijlstra A.A., Szczerba R., 1998, A&A 329, 265
Goodrich R.W., Dahari O., 1985, ApJ 289, 342
Gorny S.K., Gesicki K., Acker A., 1997, In: Habing H.J.H., Lamers G.L.M. (eds.), XXX, Kluwer Academic Publishers, Dordrecht/Boston/London, p. 230
Gorny S.K., Stasinska G., Tylenda R., 1997, A&A 318, 256
Gutierrez-Moreno A., Moreno H., Cortes G., 1985, PASP 97, 397
Harrington J.P., Borkowski K.J., Tsvetanov Z., 1995, ApJ 439, 264
Hyung S., 1994, ApJS 90, 119
Hyung S., Aller L.H., Feibelman W.A., 1994, PASP 106, 745
Kaler J.B., 1976, ApJ 210, 113
Kaler J.B., 1983, ApJ 264, 594
Leuenhagen U., Hamann W.-R., Jeffery C.S., 1996, A&A 312, 167
Manchado A., Pottasch S.R., 1989, A&A 222, 219
Mendez R.H., Herrero A., Manchado A., Kudritzki R.P., 1991, A&A 252, 265
Mendez R.H., Kudritzki R.P., Herrero A., 1992, A&A 260, 329
Mendoza, 1983, In: Habing H.J.H., Lamers G.L.M. (eds.) Proceedings of IAU Symposium 180, Planetary Nebulae. Kluwer, Dordrecht
Oke, 1990, AJ 99, 1621
Osterbrock D.E., 1989, Astrophysics of gaseous nebulae and active galactic nuclei. University Science Books
Peimbert M., Torres-Peimbert S., 1971, Bol. Obs. Ton. y Tac. No. 36, 6, 21
Perinotto M., Purgathofer A., Pasquali A., Patriarchi P., 1994, A&AS 107, 481
Rudy R.J., Cohen R.D., Rossano G.S., et al., 1991, ApJ 380, 151
Sabbadin F., 1980, A&A 84, 216
Sabbadin F., 1984, MNRAS 209, 889
Schönberner D., 1997, In: Habing H.J.H., Lamers G.L.M. (eds.) Proceedings of IAU Symposium 180, Planetary Nebulae. Kluwer, Dordrecht, p. 379
Schwarz H.E., Corradi R.L.M., Melnick J. 1992, A&AS 96, 23
Stanghellini, 1997, In: Habing H.J.H., Lamers G.L.M. (eds.) Proceedings of IAU Symposium 180, Planetary Nebulae. Kluwer, Dordrecht, p. 319
Stanghellini L., Kaler J.B., Shaw R.A., 1994, A&A 291, 604
Stasinska G., Gorny S.K., Tylenda R., 1997, A&A 327, 736
Surendiranath R., Kameswara Rao N., 1995, MNRAS 275, 685
Zhang C.Y., 1993, ApJ 410, 239
Zhang C.Y., 1995, A&AS 111, 27
Zhang C.Y., Kwok S., 1993, ApJS 88, 137